Gene Conversion Facilitates the Adaptive Evolution of Self-Resistance in Highly Toxic Newts

Kerry L. Gendreau (ID),*,[1] Angela D. Hornsby,[1,2] Michael T.J. Hague,[3] and Joel W. McGlothlin[1]

[1]Department of Biological Sciences, Virginia Tech, Blacksburg, VI, USA
[2]Philip L. Wright Zoological Museum, Division of Biological Sciences, University of Montana, Missoula, MT, USA
[3]Division of Biological Sciences, University of Montana, Missoula, MT, USA

*Corresponding author: E-mail: kerryg@vt.edu.
Associate editor: John Parsch

Abstract

Reconstructing the histories of complex adaptations and identifying the evolutionary mechanisms underlying their origins are two of the primary goals of evolutionary biology. *Taricha* newts, which contain high concentrations of the deadly toxin tetrodotoxin (TTX) as an antipredator defense, have evolved resistance to self-intoxication, which is a complex adaptation requiring changes in six paralogs of the voltage-gated sodium channel (Na$_v$) gene family, the physiological target of TTX. Here, we reconstruct the origins of TTX self-resistance by sequencing the entire Na$_v$ gene family in newts and related salamanders. We show that moderate TTX resistance evolved early in the salamander lineage in three of the six Na$_v$ paralogs, preceding the proposed appearance of tetrodotoxic newts by $\sim$100 My. TTX-bearing newts possess additional unique substitutions across the entire Na$_v$ gene family that provide physiological TTX resistance. These substitutions coincide with signatures of positive selection and relaxed purifying selection, as well as gene conversion events, that together likely facilitated their evolution. We also identify a novel exon duplication within Na$_v$1.4 encoding an expressed TTX-binding site. Two resistance-conferring changes within newts appear to have spread via nonallelic gene conversion: in one case, one codon was copied between paralogs, and in the second, multiple substitutions were homogenized between the duplicate exons of Na$_v$1.4. Our results demonstrate that gene conversion can accelerate the coordinated evolution of gene families in response to a common selection pressure.

Key words: gene conversion, adaptation, coevolutionary arms races, molecular evolution, newts, toxin resistance.

Introduction

Fitting evolutionary models to molecular sequences in a phylogenetic context can help piece together the key steps in adaptive evolution and uncover the relative contributions of selection and other evolutionary mechanisms to adaptive phenotypic evolution (Smith et al. 2020). Comparative studies of convergence, or the repeated evolution of characters within different lineages undergoing the same environmental challenges, provide powerful evidence of both adaptation and connections between genetic and phenotypic change (Losos 2011). Investigations into the molecular basis of convergence have revealed multiple occurrences of parallelism, where different lineages have evolved changes within the same proteins, and occasionally at the same amino acid sites, in response to shared selective pressures, such as insects that have evolved the ability to feed on toxic plants (Zhen et al. 2012) and populations of ducks and humans living at high elevations (Graham and McCracken 2019). Such patterns support important roles for both positive selection and constraint in the origin of complex adaptations (reviewed by Storz 2016).

Resistance to tetrodotoxin (TTX), a potent neurotoxin, has evolved convergently in several distantly related organisms, including pufferfish, snakes, and newts (reviewed by Soong and Venkatesh 2006; Toledo et al. 2016), and therefore offers an ideal system to investigate the molecular basis of adaptive evolution (Arbuckle et al. 2017). The genetic basis of TTX resistance, which is well established in tetrodotoxic puffer fish (Jost et al. 2008) and in snakes that consume TTX-bearing prey (Geffeney et al. 2002; Feldman et al. 2012; McGlothlin et al. 2014, 2016), involves amino acid substitutions in the toxin's target, voltage-gated sodium channels (Na$_v$). Although Na$_v$ are commonly abbreviated as *SCNA* genes and Na$_v$ proteins, hereafter, we simplify this nomenclature by abbreviating both as Na$_v$. Na$_v$ channels are responsible for the initiation and propagation of action potentials in excitable cells and are composed of four domains (DI–DIV), each comprising six transmembrane helices and a pore-loop region (the P-loop; Fux et al. 2018). The four P-loops, one in each domain, form a pore within the membranes of excitable cells to selectively allow sodium ions to cross when the channel is open. TTX exerts its effects by binding to the P-loops of sensitive channels and preventing sodium entry into

Article

Fast Track

cells, thus blocking action potentials. Gene duplication events have resulted in six Na$_v$ paralogs, each with tissue-specific expression, that are shared across all tetrapods (table 1), with additional lineage-specific duplications occurring in amniotes (Widmark et al. 2011; Zakon 2012). Because the structure of these paralogs is highly conserved, each has the potential to be blocked by TTX if it lacks resistance-conferring substitutions.

Species that possess or consume TTX must either have a full complement of resistant paralogs or otherwise shield sodium channels from contact with the toxin. Indeed, resistant substitutions are present in all eight of the Na$_v$ genes within the genomes of multiple species of TTX-bearing pufferfish (from the family Tetraodontidae; Jost et al. 2008) and in six of the nine Na$_v$ genes in *Thamnophis sirtalis* snakes that consume TTX-bearing *Taricha* newts (McGlothlin et al. 2014; Perry et al. 2018). The three brain channels Na$_v$1.1, Na$_v$1.2, and Na$_v$1.3 of snakes remain TTX sensitive, but presumably are protected from TTX by the blood-brain barrier (McGlothlin et al. 2014). In snakes, the evolution of extreme TTX resistance appears to follow a predictable, stepwise substitution pattern across TTX-exposed members of the Na$_v$ gene family, with substitutions in heart and peripheral nerve channels preceding those in the muscle channel gene, Na$_v$1.4, which evolves resistance only in snakes locked in coevolutionary arms races with highly tetrodotoxic amphibian prey (Feldman et al. 2012; McGlothlin et al. 2016; Perry et al. 2018).

Less is known about the evolutionary history of TTX resistance in *Taricha* newts, the highly toxic coevolutionary partner of *Thamnophis* (Brodie and Brodie 1990; Brodie et al. 2002; Williams et al. 2010; Hague et al. 2020). The extreme toxicity of *Taricha*, which has been elaborated by the ongoing coevolutionary arms race with garter snakes, builds upon lower levels of toxicity that evolved ~30 Ma within "modern" newts (tribe Molgini; Hanifin and Gilly 2015; divergence date estimated by Hime et al. 2021). The evolution of toxicity necessitates the evolution of toxin autoresistance so that a prey species is not incapacitated by its own antipredator defense (Jost et al. 2008; Toledo et al. 2016; Tarvin et al. 2017; Márquez et al. 2019). Understanding the timing and details of this autoresistance can shed light on the genetic processes underlying the predator-prey arms race. Hanifin and Gilly (2015) compared the sequences of one sodium channel gene, the muscle paralog Na$_v$1.4, across several salamander species and identified substitutions in the P-loops of DIII and DIV that provide extreme TTX resistance to the muscles of TTX-bearing newts. Importantly, the sister group of these toxic newts had substitutions in the same gene providing more moderate resistance, indicating that the evolution of autoresistance in a common ancestor paved the way for the evolution of extreme toxicity. More recently, Vaelli et al. (2020) used transcriptome sequencing to characterize the genetic basis of physiological resistance to TTX in *Taricha granulosa* and identified substitutions within TTX-binding regions in the other five Na$_v$ paralogs, many of which occur within the P-loop of DI. However, because it is unknown whether other salamander species possess TTX resistance in these paralogs, the order and timing of the evolutionary

events leading to autoresistance in toxic newts are still unknown. Furthermore, no studies to date have applied evolutionary models to test for the relative importance of mechanisms such as positive selection, relaxed constraint, and interlocus gene conversion in the evolution of newt TTX resistance.

Here, we trace the evolutionary history of the entire Na$_v$ gene family across the salamander phylogeny to show the order in which resistant substitutions appeared. Using published genome sequences and newly generated sequence data, we characterize the genomic structure of Na$_v$ genes in newts and their relatives, inferring the timing of resistant substitutions leading to the extreme TTX resistance observed across all Na$_v$ paralogs in *Taricha* newts (Vaelli et al. 2020). We estimate rates of synonymous and nonsynonymous substitution to identify positive selection. In addition, we assess the potential of nonallelic gene conversion, a process by which sequence is copied from one paralog to another (Chen et al. 2007), to act as a source of adaptive variation. Combining these data provides insight into the evolutionary mechanisms underlying the origin of a uniquely potent chemical defense.

Results

Genomic Structure of Voltage-Gated Sodium Channels

We used targeted sequence capture to characterize Na$_v$ sequences from the genomes of five salamander species (order Urodela), including three TTX-bearing newts (family Salamandridae, subfamily Pleurodelinae, tribe Molgini), *Notophthalmus viridescens*, *Taricha torosa*, and *Taricha granulosa* ($n = 3$ diploid individuals of each species), and two salamanders that do not possess TTX, *Cryptobranchus alleganiensis* (Crypotobranchidae) and *Plethodon cinereus* (Plethodontidae, $n = 2$ each). We also identified Na$_v$ sequences within two publicly available salamander genome sequences: *Ambystoma mexicanum* (Ambystomatidae; Smith et al. 2019; AmexG.v6 assembly) and *Pleurodeles waltl* (Salamandridae; Elewa et al. 2017) and a full-body transcriptome from the fire salamander *Salamandra salamandra* (Salamandridae; Goedbloed et al. 2017; BioProject accession number PRJNA607429), all three of which appear to lack TTX (Hanifin 2010). The split between *Cryptobranchus* (suborder Cryptobranchoidea) and all the other salamanders in our study (members of suborder Salamandroidea) represents the most ancient division in the phylogeny of extant salamanders (~160 Ma; Hime et al. 2021).

We identified six Na$_v$ genes in the genomes of all salamander species, which is consistent with observations in other amphibians (Zakon et al. 2011). Hereafter, we use the exon delineation introduced in Widmark et al. (2011), where domain I (DI) is encoded by exons 2-9, domain II (DII) is encoded by exons 13-16, domain III (DIII) is encoded by exons 18-23, and domain IV (DIV) is encoded by exons 25-26. We obtained near full-length assemblies for all paralogs (supplementary table S1, Supplementary Material online); however, a few exons containing TTX-binding sites, including exon 15 (encoding the DII P-loop) of Na$_v$1.2 from *N. viridescens* and

Table 1. Nomenclature for Voltage-Gated Sodium Channel Genes.

Gene Name	Protein Name	Tissue Expression[a]
SCN1A	$Na_V1.1$	Brain
SCN2A	$Na_V1.2$	Brain
SCN3A	$Na_V1.3$	Brain
SCN4A	$Na_V1.4$	Muscle
SCN5A	$Na_V1.5$	Heart
SCN8A	$Na_V1.6$	Brain/peripheral nervous system

[a]Patterns of tissue expression are inferred from studies of gene orthologs in mammals (reviewed in Yu and Catterall [2003]).

exon 22 (encoding part of the DIII P-loop) of $Na_V1.2$ for several newt species, were missing from our assemblies. Polymorphism was rare in our assemblies and we observed few nonsynonymous mutations within the newt genomes, but we found slightly elevated polymorphism in *N. viridescens* relative to other species (supplementary table S2, Supplementary Material online). No heterozygosity or nonsynonymous polymorphisms were observed in any of the known TTX-binding P-loop regions within any of the species sequenced for this study.

Synteny of Na_V genes in *A. mexicanum* is conserved relative to other tetrapods (supplementary fig. S1, Supplementary Material online), which allowed us to use the *A. mexicanum* sequences as a baseline to confidently identify Na_V paralogs in all species. Three of the paralogs, $Na_V1.1$, $Na_V1.2$, and $Na_V1.3$ are arrayed in tandem on *A. mexicanum* chromosome 9, with $Na_V1.2$ inverted relative to its neighboring paralogs (table 2 and supplementary fig. S1, Supplementary Material online). The additional three paralogs, $Na_V1.4$, $Na_V1.5$, and $Na_V1.6$, are each located on separate chromosomes (table 2). In the gene family tree built from amino acid sequences, all salamander Na_V proteins formed a monophyletic clade (bootstrap support >98%) with the corresponding orthologs from the genomes of the frogs *Xenopus tropicalis* and *Nanorana parkeri*, which we included as outgroups (fig. 1). The gene family tree constructed from the nucleotide-coding sequences of these genes yielded a similar topology, with each salamander Na_V ortholog forming a monophyletic clade. However, in the nucleotide gene family tree, the three *X. tropicalis* nerve channels $Na_V1.1$, $Na_V1.2$, and $Na_V1.3$ formed a monophyletic clade that is distinct from the salamander sequences (bootstrap support 86%; supplementary fig. S2, Supplementary Material online). The same tree topology was resolved when partitioning for the third codon position (see Supplementary Material online on Dryad).

Partial Duplication of $Na_V1.4$ and Evolution of TTX Resistance in Duplicated Domains

Our search of the *A. mexicanum* genome revealed a partial tandem duplication of the 3′ end of the $Na_V1.4$ gene, including the full coding region of exon 26, located ~180,000 base pairs downstream of the full-length $Na_V1.4$ gene on the same DNA strand (table 2). Both exon 26 copies are similar in length to each other and to exon 26 of other paralogs, encoding open reading frames of approximately 390 amino acids without introduced stop codons. Exon 26 is the 3′-terminal

exon of the $Na_V1.4$ gene and encodes the TTX-binding P-loop region of DIV. Hereafter, we refer to the duplicate exons as 26a (more proximal to exon 25) and 26b (more distal to exon 25) and duplicate P-loop regions as DIVa (more proximal to exon 25) and DIVb (more distal to exon 25). We also found this duplicated exon in $Na_V1.4$ orthologs within the genomes of salamanders *P. cinereus*, *Ple. waltl*, *N. viridescens*, *T. torosa*, and *T. granulosa* and in published transcriptomes of *Tylototriton wenxianensis* and *Bolitoglossa vallecula*, but not in the transcriptome of *Hynobius retardatus* or in the genomes of *C. alleganiensis* or the frogs *X. tropicalis* or *Nan. parkeri*. This pattern suggests that the duplication event likely took place after the split of Cryptobranchoidea and Salamandroidea (fig. 2). Within the *S. salamandra* transcriptome, we found four unique RNA sequences transcribed from the $Na_V1.4$ locus, with alternative splicing of exon 17 and alternative encoding of either exon 26a or 26b. Genome-mapped reads of multitissue transcriptomes of *A. mexicanum* (Bryant et al. 2017; Caballero-Pérez et al. 2018; Nowoshilow et al. 2018) indicate that these alternative transcripts have similar expression profiles across various tissues. Taken together, these observations provide evidence that the duplication of exon 26 led to the creation of functional splice variants in these salamanders.

Although numerous nonsynonymous substitutions differentiated the duplicated $Na_V1.4$ exon 26 sequences relative to the original sequences within each genome, we found that identical substitutions conferring extreme TTX-resistance to toxic newts (Hanifin and Gilly 2015) were present in both exons from the genomes of all three TTX-bearing newts but not in other, less toxic salamander species (fig. 2). Also consistent with the results of Hanifin and Gilly (2015), we found resistant substitutions conferring moderate TTX resistance in exon 26a of *Ple. waltl*, *Tyl. wenxianensis*, and *S. salamandra*; however, we observed no resistant substitutions in exon 26b outside of the toxic newt clade.

Evolution of TTX Resistance in Salamanders

We characterized levels of TTX resistance in each Na_V paralog as extreme, moderate, and TTX-sensitive based on previous site-directed mutagenesis experiments in which substitutions were introduced to TTX-sensitive Na_V channels and cross-membrane Na^+ current was measured in vitro in the presence and absence of TTX (table 3). Our results confirm that *T. granulosa* has six paralogs with extreme TTX resistance (table 3 and fig. 3). Our findings are consistent with those reported by Vaelli et al. (2020) with one exception: we associate DIV (encoded by exon 26) substitutions A1529G, G1533V, and G1533A with $Na_V1.1$ and Q1524E, G1533R, and G1533Q with $Na_V1.2$ based on synteny mapping (supplementary fig. S1, Supplementary Material online), gene trees (fig. 1 and supplementary fig. S2, Supplementary Material online), and a phylogeny created from a coding sequence alignment of exon 26 (supplementary fig. S3, Supplementary Material online), whereas the previous study reversed these assignments. We also show that substitutions with extreme TTX resistance are present in all six Na_V paralogs in two other species of highly toxic newt, *T. torosa* and *N. viridescens*, indicating

Table 2. Locations of Na$_v$ Genes in the *Ambystoma mexicanum* AmexG.v6 Genome Assembly.

Gene	Chromosome	Start	End	Strand	Length (bp)
Na$_v$1.1	9q	503,107,904	503,797,933	+	690,029
Na$_v$1.2	9q	507,685,503	508,688,108	−	1,002,605
Na$_v$1.3	9q	509,830,827	510,576,927	+	746,100
Na$_v$1.4	13q	113,343,821	115,707,581	+	2,363,760
Na$_v$1.4 exon 26b	13q	115,891,071	115,892,251	+	1,180
Na$_v$1.5	2p	562,159,042	563,030,267	−	871,225
Na$_v$1.6	3q	465,212,114	466,692,047	−	1,479,933

that the common ancestor of these three species possessed extreme TTX resistance. Many of the substitutions in toxic newts parallel those found in TTX-bearing fish and in snakes that consume tetrodotoxic amphibians (table 3).

No salamander species outside the clade of highly toxic newts possessed a full complement of TTX-resistant Na$_v$ paralogs, indicating that the evolution of full physiological resistance coincided with the origin of extreme toxicity. However, we found at least three paralogs with moderate or extreme TTX resistance in all salamander species we examined, indicating that the evolution of TTX resistance in newts built upon more ancient changes that first appeared in their nonnewt relatives. Substitutions conferring moderate or extreme resistance were observed within the heart channel Na$_v$1.5 and brain/nerve channels Na$_v$1.1 and Na$_v$1.6 of all salamander species, with additional resistance-conferring substitutions evolving within TTX-bearing newts. As first shown by Hanifin and Gilly (2015), moderate resistance was present in the skeletal muscle channel Na$_v$1.4 of *S. salamandra* and *Ple. waltl*, but not in the three other salamander species we examined. Although our outgroup, the frog *X. tropicalis*, also contained a highly resistant substitution in Na$_v$1.2, we found no evidence for resistance in this paralog in any salamanders outside of tetrodotoxic newts.

Based on our ancestral sequence reconstructions, the most recent common ancestor of all salamanders had three TTX-resistant sodium channels: Na$_v$1.1 (brain, moderately resistant), Na$_v$1.5 (heart, highly resistant), and Na$_v$1.6 (brain/peripheral nerves, moderately resistant; fig. 3 and supplementary figs. S4–S9, Supplementary Material online). Moderate resistance in the muscle channel Na$_v$1.4 appeared between 75 and 130 Ma, after the divergence of Ambystomatidae and Salamandridae (the family consisting of true salamanders and newts; Hanifin and Gilly 2015). This gain in muscle resistance coincided with the appearance of two highly resistant substitutions in DI of Na$_v$1.5, which are present in all Salamandridae. Extreme TTX resistance across all Na$_v$ paralogs evolved more recently, occurring approximately 30 Ma, after the split between primitive newts, which include *Pleurodeles*, and modern newts (Hime et al. 2021), which include all TTX-bearing species. Over this time period, TTX resistance evolved in Na$_v$1.2 and Na$_v$1.3, and multiple additional resistant mutations appeared and became fixed in Na$_v$1.1, Na$_v$1.4, and Na$_v$1.6.

Selective Regimes and Evolutionary Rates

In order to characterize the selective regimes acting on Na$_v$ genes, we used the codeml program in PAML (Yang 2007) to fit models of selection to Na$_v$ codon alignments and compared nested models using likelihood ratio tests (LRTs). We tested for site-specific positive selection within all amphibians by comparing two sets of nested models: one set using a discrete distribution of ω values either with or without positive selection (M1a vs. M2a; Yang et al. 2005); and another set fitting a continuous distribution of ω values under purifying selection only, or adding categories of unconstrained evolution and positive selection (M7 vs. M8 and M8a vs. M8; Yang et al. 2000). Parameter estimates and LRT results for site models are summarized in supplementary table S3, Supplementary Material online. To test for selection within toxic newts, we fit branch (Yang 1998) and branch-site models (Zhang et al. 2005) to our data sets, which allowed ω to vary both among codon sites and between toxic newts and other amphibians (summarized in supplementary table S4, Supplementary Material online).

All models estimated relatively low ratios of nonsynonymous to synonymous substitution (d_N/d_S, or ω ratios) for all Na$_v$ paralogs (average ω ratios from branch models ranged from 0.05 to 0.23), indicating pervasive purifying selection. Based on LRTs comparing one ω-value models (which allow only for one ω value across the entire phylogeny) to branch models (allowing for a different ω ratio in the toxic newt clade relative to other amphibians), we found that ω ratios were significantly ($P < 0.01$) higher in toxic newts for Na$_v$1.1, Na$_v$1.3, and Na$_v$1.4 and nonsignificant ($P > 0.01$) for Na$_v$1.2, Na$_v$1.5, and Na$_v$1.6 (fig. 4A and supplementary table S4, Supplementary Material online). The largest difference in ω ratios in the branch test was observed for the muscle channel Na$_v$1.4 (newt $\omega = 0.23$; all salamanders $\omega = 0.10$), which appears to be due to both an increase in the proportion of unconstrained sites as well as a larger number of estimated sites undergoing positive selection (fig. 4B). However, the posterior probability support for positive selection at many of these sites was low, and LRTs from branch-site models indicated significant evidence for a shift in positive selection only in paralog Na$_v$1.3 (supplementary tables S4 and S5, Supplementary Material online).

Our site and branch-site models identified a number of TTX-binding sites with elevated ω ratios (table 4 and supplementary tables S5 and S6, Supplementary Material online). Because of the small number of species in our study, we had low power to detect statistically significant positive selection (Yang et al. 2000; Anisimova et al. 2001; Kosakovsky Pond and Frost 2005), and the posterior probabilities provided low-to-moderate support for positive selection at most sites. We also
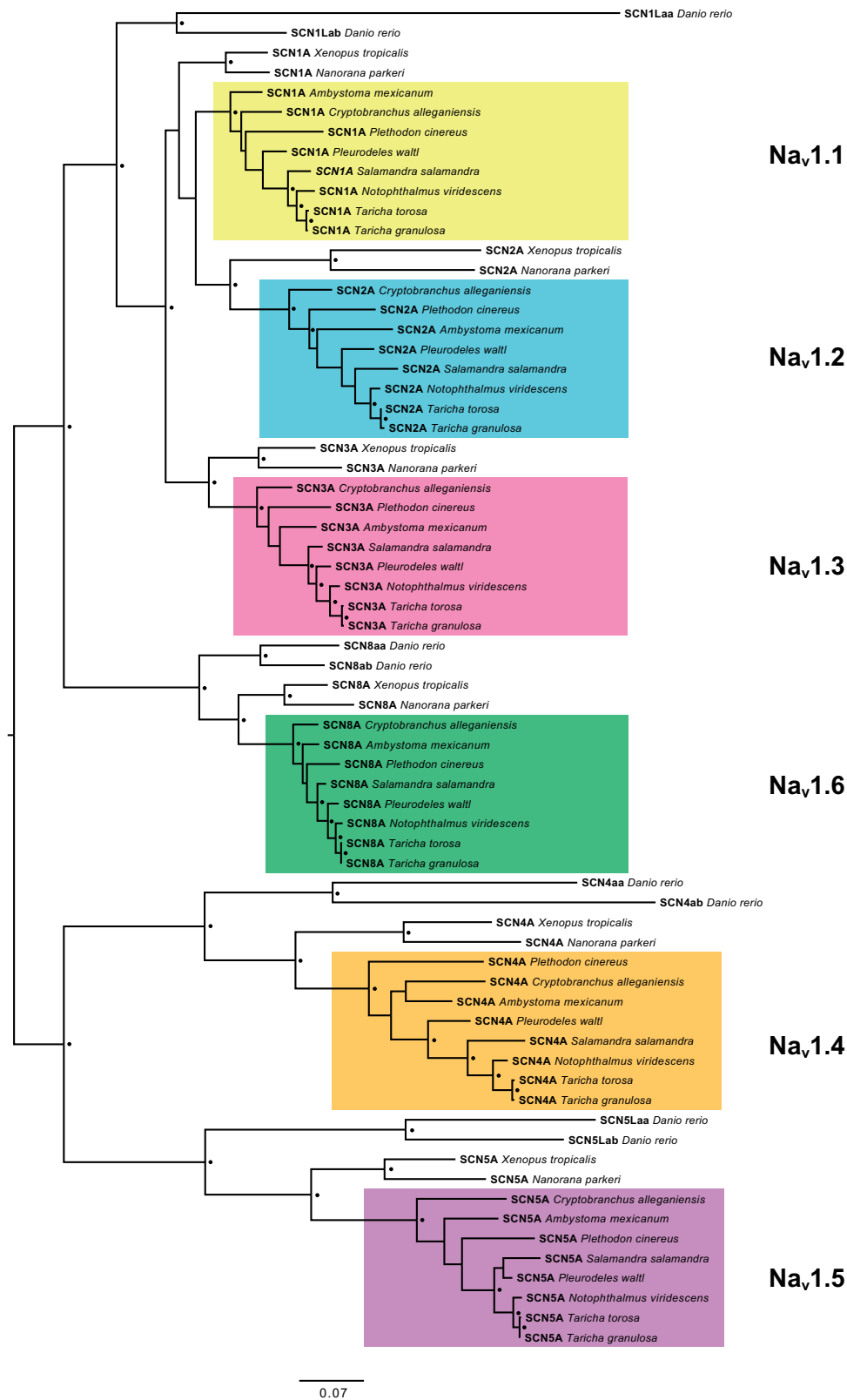
Fig. 1. Evolutionary relationships among salamander voltage-gated sodium channels. Midpoint rooted maximum likelihood tree constructed from alignment of 2,188 amino acids from full coding sequence translations of salamander sodium channel genes, including sequences from two frogs (*Nanorana parkeri* and *Xenopus tropicalis*) and one fish (*Danio rerio*) as outgroups. Black circles indicate nodes with >90% bootstrap support.

note that the false positive rates of site selection models can be inflated due to gene conversion events (Casola and Hahn 2009), among-site variation in d_S (Kosakovsky Pond and Frost 2005), and multinucleotide mutations (Venkat et al. 2018). However, results were consistent between the M2a and M8 models, and the codons that were identified suggest that
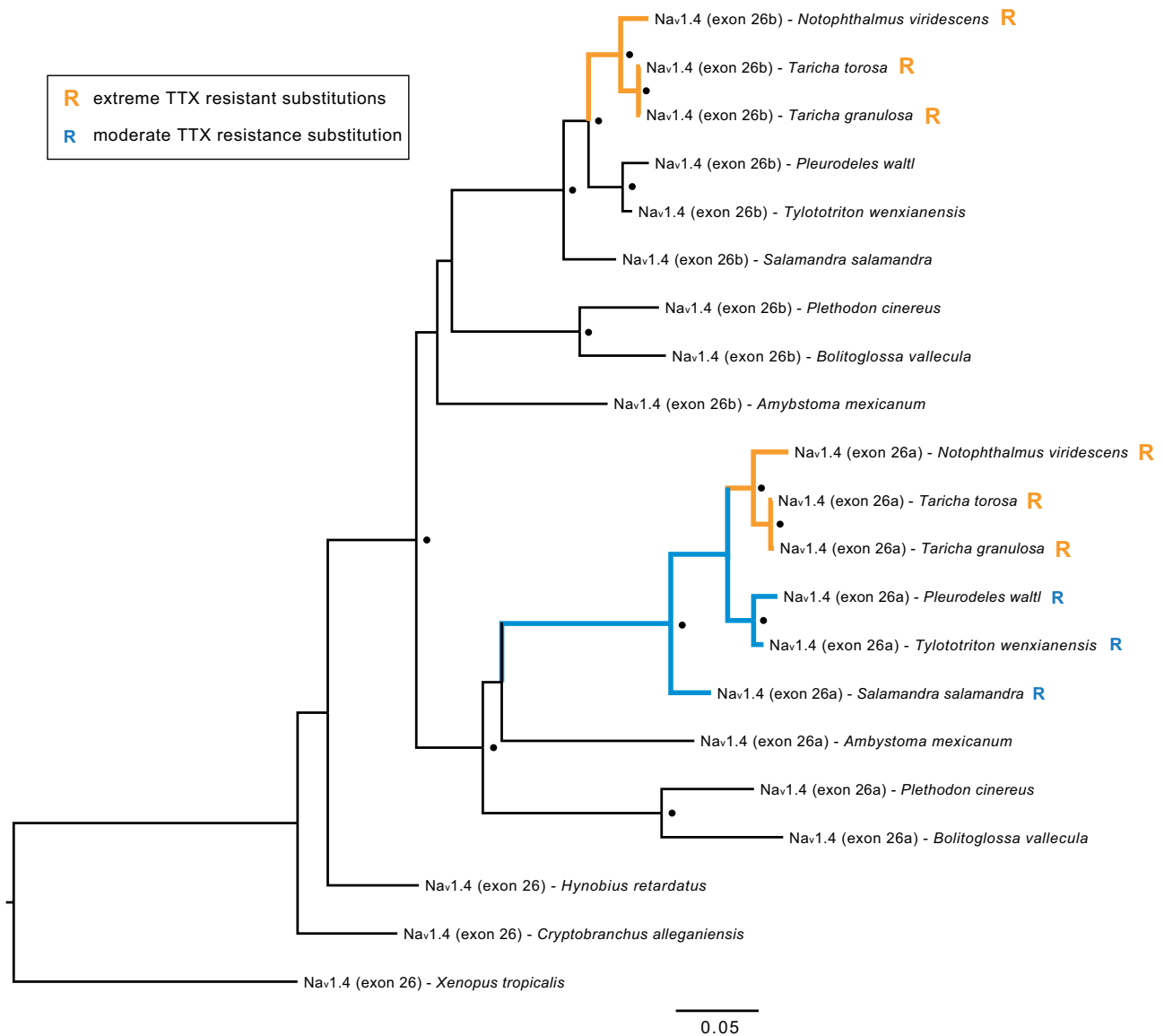
FIG. 2. Ancestral duplication and convergent evolution of TTX resistance in $Na_v1.4$ terminal exon 26. Maximum likelihood tree constructed from 1,050 bp nucleotide alignment of $Na_v1.4$ exon 26 identified in salamander genomes and transcriptomes. "Exon 26a" and "exon 26b" in tip labels refer to the exon copy more proximal and more distal to exon 25, respectively. Black circles indicate node bootstrap support >95%. "R" at tips indicates the presence of substitutions conferring extreme (orange) and moderate (blue) TTX resistance. The same tree topology was resolved using an alignment of amino acids translations of these sequences.

positive selection may have been important for observed substitutions in TTX-binding regions.

Within the brain channels $Na_v1.1$, $Na_v1.3$, and $Na_v1.6$, putative positive selection was detected by site models at site 401 within the DI P-loop, indicating selection acting across all salamanders rather than specifically within toxic newts (table 4). Replacement of the aromatic amino acid at site 401 with a nonaromatic amino acid can substantially impact TTX-binding capacity (Leffler et al. 2005; Venkatesh et al. 2005; Vaelli et al. 2020), and we observed nonaromatic substitutions at this site within all brain channels of highly toxic newts (fig. 3 and table 3). The codon sequence for site 401 was variable across many salamanders lacking TTX; however, almost all of the nonsynonymous changes observed outside of TTX-

bearing newts were biochemically conservative (both phenylalanine and tyrosine are aromatic and do not affect TTX binding; Sunami et al. 2000), with the exception of the 401A observed in *P. cinereus* $Na_v1.1$. This conservative variation likely contributes to the signal of diversifying selection acting on this codon in less toxic salamander lineages. Site models also suggested positive selection acting on site 1533 in DIV of $Na_v1.1$ and $Na_v1.2$ (table 4). Although the substitutions present at site 1533 in these newt paralogs have not been tested experimentally for their effects on TTX binding, Maruta et al. (2008) showed that a G1533T substitution at this site led to a moderate (~2- to 3-fold) decrease in TTX-binding affinity, and substitutions at this site are common in TTX-resistant channels (Geffeney et al. 2005; Jost et al. 2008;

Table 3. List of TTX Resistance-Conferring Substitutions Observed in Salamanders.

Substitution[a]	Tetrodotoxic Newts	Nontetrodotoxic Salamanders	Pufferfish and Snakes[b]	Fold Change in TTX Sensitivity	Resistance Category	Citation
Y401C (DI)	$Na_v1.1$ $Na_v1.2$	$Na_v1.5$	Pufferfish: $Na_v1.4a$ $Na_v1.5La$ $Na_v1.5Lb$	~2,500×	Extreme	Venkatesh et al. (2005); Jost et al. (2008)
Y401A (DI)	$Na_v1.1$ $Na_v1.3$ $Na_v1.6$	$Na_v1.1$	Pufferfish: $Na_v1.1La$ $Na_v1.6b$	>600×	Extreme	Jost et al. (2008); Vaelli et al. (2020)
Y401S (DI)	$Na_v1.5$	$Na_v1.5$	—	~7,000×	Extreme	Leffler et al. (2005)
D1532S (DIV) G1533D (DIV)	$Na_v1.4$		Snake: $Na_v1.4$	—	Extreme[c]	Feldman et al. (2012); Hanifin and Gilly (2015)
E758D (DII)	—	$Na_v1.5$	Pufferfish: $Na_v1.4b$	~3,000×	Extreme	Bricelj et al. (2005)
M1240T (DIII)	$Na_v1.1$ $Na_v1.4$	$Na_v1.1$ $Na_v1.5$	Pufferfish: $Na_v1.1La$ $Na_v1.1Lb$ $Na_v1.4a$ $Na_v1.4b$	~15×	Moderate	Jost et al. (2008)
V1233I (DIII)	$Na_v1.6$	$Na_v1.6$	Snake: $Na_v1.6$	~2×	Moderate	McGlothlin et al. (2014); Vaelli et al. (2020)
I1525V (DIV)	$Na_v1.6$	$Na_v1.5$ $Na_v1.6$	Snake: $Na_v1.6$	~2×	Moderate	Geffeney et al. (2005); McGlothlin et al. (2014); Vaelli et al. (2020)
I1525S (DIV)	$Na_v1.4$	$Na_v1.4$		—	Moderate[c]	Hanifin and Gilly (2015)
I1525T (DIV)	—	$Na_v1.4$ $Na_v1.5$		~7.7×	Moderate	Du et al. (2009)

[a]Amino acid sites are in reference to rat $Na_v1.4$ (accession number AAA41682).
[b]Parallel substitutions in Na_v channels of TTX-bearing pufferfish and in snakes that consume TTX-bearing prey.
[c]Resistance category determined from action potentials recorded from salamander muscle fibers.

Feldman et al. 2012; McGlothlin et al. 2016), suggesting that these nonsynonymous changes likely also reduce TTX-binding affinity in newts.

Within the toxic newt lineage, we identified putative positive selection acting on three known TTX-binding sites: 1240 and 1532 in DIII and DIV of muscle channel $Na_v1.4$ and 1529 in DIV of brain channel $Na_v1.1$ (table 4). In $Na_v1.4$, sites 1240 and 1532 contain resistance-conferring substitutions exclusively within toxic newts and these substitutions have been associated with extreme TTX resistance in *Taricha* muscle fibers (Hanifin and Gilly 2015). In $Na_v1.1$, site 1529 encodes part of the Na^+ selectivity filter (comprised interacting amino acids DEKA—sites 400, 755, 1237, and 1529), which is highly conserved across Na_v paralogs. An A1529G substitution (resulting in a DEKG filter) is present in $Na_v1.1$ of *A. mexicanum* and all members of the toxic newt clade. Although this substitution does not appear to affect Na^+ selectivity or to be sufficient in preventing TTX from binding (Jost et al. 2008), it may alter channel firing properties, as this A1529G substitution resulted in substantially higher Na^+ currents relative to the wild-type when introduced into a mammalian $Na_v1.4$ channel (Jost et al. 2008). The same alanine to glycine substitution has been observed in Na_v channels of TTX-bearing flatworms (Jeziorski et al. 1997) and pufferfish (Jost et al. 2008), which suggests that it may play a role in TTX resistance in these organisms.

Outside of TTX-binding regions, we found evidence for putative positive selection in similar regions across multiple Na_v paralogs (supplementary tables S5 and S6, Supplementary Material online). For $Na_v1.4$, the majority of sites under positive selection reside in terminal exon 26a that encodes the DIVa P-loop (exon 26b was excluded from this analysis due to its absence in some species). For most other paralogs, the largest clusters of sites with elevated d_N/d_S ratios were within the DI L5 turret (the extracellular loop upstream of the DI P-loop, encoded by exons 6 and 7) and the DIII L5 turret upstream of the DIII P-loop encoded by exon 21.

These sites may facilitate interaction with other proteins, or alternatively, some of these sites identified by the branch-site model may be selected to compensate for biochemical changes produced by TTX-resistant mutations.

Gene Conversion Events

We also tested for evidence of nonallelic gene conversion as a mechanism of sequence evolution contributing to adaptive evolution in Na_v genes using the program GENECONV. Nonallelic or ectopic gene conversion results from an inter-locus exchange of DNA that can occur between closely related sequences during double-stranded break repair (Hansen et al. 2000). GENECONV uses the information in a multiple sequence alignment to identify regions of similarity shared between two sequences that is higher than expected by chance based on comparisons to permuted alignments (Sawyer 1989). We selected this program to detect gene conversion because of its low false positive rates and robustness to shifts in selective pressure (Posada and Crandall 2001; Bay and Bielawski
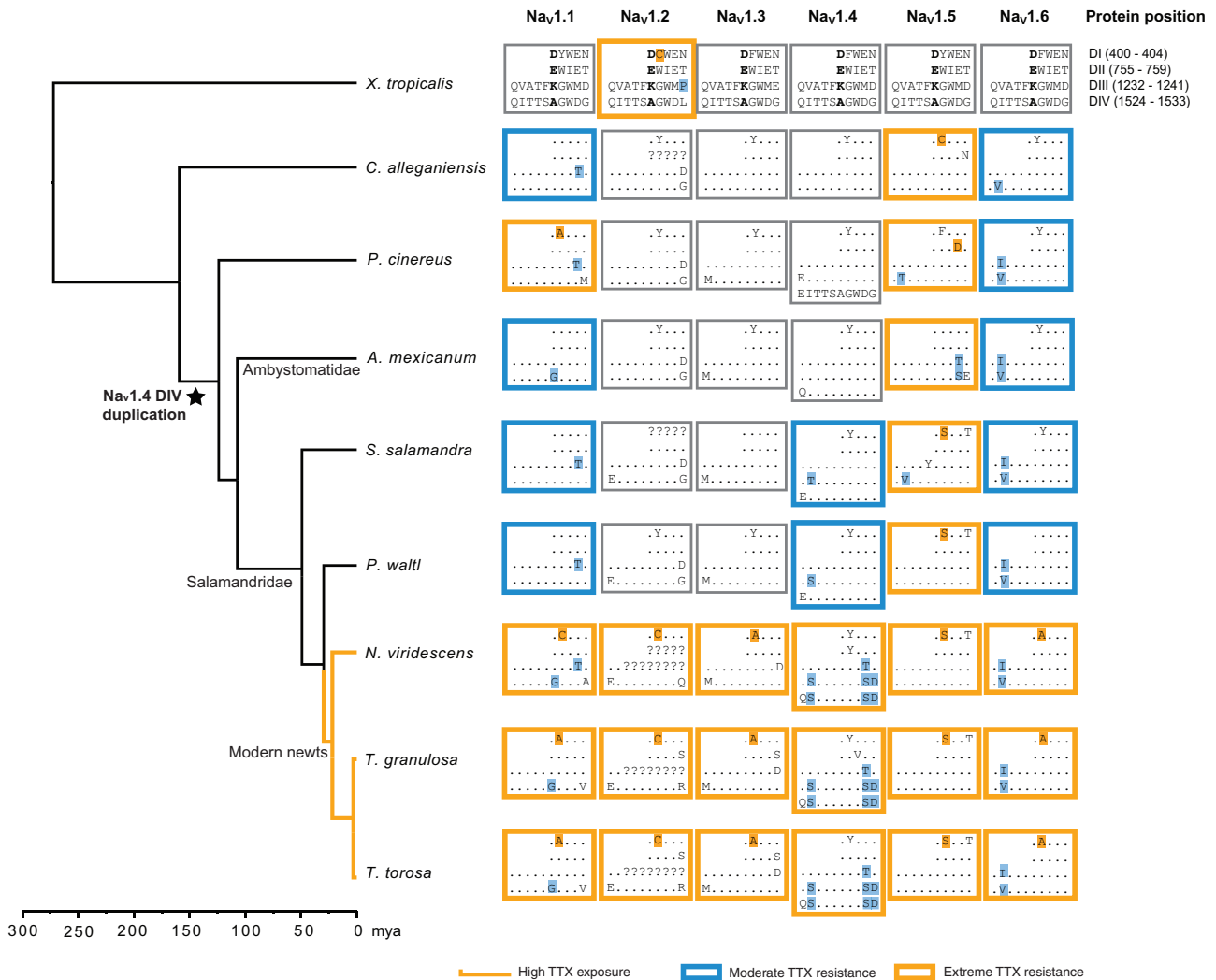
FIG. 3. Distribution of TTX-resistance conferring substitutions in salamander voltage-gated sodium channels. Toxic newt species are indicated with orange branches ("High TTX exposure"). Amino acids associated with Na$^+$ selectivity (400D, 755E, 1237K, 1529A) are shown in bold. Dots indicate identity with consensus sequences. Blue boxes indicate paralogs inferred to have moderate ($\sim$2- to 15-fold) resistance, orange boxes indicate paralogs with extreme ($>$300-fold) resistance, and gray boxes indicate paralogs without resistance or with insufficient sequence data. Substitutions known to confer TTX resistance are highlighted with respective colors. Extreme resistance in a paralog can result from the presence of one highly resistant substitution or the combination of multiple moderately resistant substitutions. Exon duplication has led to an additional TTX-binding domain (DIVb) in Na$_v$1.4 of all salamanders except *Cryptobranchus alleganiensis*. We did not identify the sequence encoding DIII of Na$_v$1.2 for any of the newts, however, Vaelli et al. (2020) report that, in *Taricha granulosa*, this domain is identical in amino acid sequence to other salamanders. Amino acid sites are in reference to rat Na$_v$1.4 (accession number AAA41682).

2011). Because nonallelic gene conversion is more likely to occur between paralogs residing on the same chromosome (Semple and Wolfe 1999; Drouin 2002; Benovoy and Drouin 2009), we limited our search to events between the tandem duplicates Na$_v$1.1, Na$_v$1.2, and Na$_v$1.3 and between exons 26a and 26b of Na$_v$1.4 within each salamander genome. Although few gene conversion events were detected within each species by GENECONV, all of the regions that were detected within *Taricha* newts contain TTX-binding sites with substitutions associated with TTX resistance, including the DIVa and DIVb P-loops of Na$_v$1.4 (fig. 5 and table 5). We observed three TTX-resistant amino acids (I1525S, D1532S, G1533D) within the DIVa and DIVb P-loops of Na$_v$1.4 in toxic newt genomes. In contrast, *Ple. waltl*, a closely related but nontetrodotoxic newt, contains one moderately TTX-resistant amino acid (I1525S) in

the DIVa P-loop and no resistant amino acids in the DIVb P-loop (fig. 5A). These differences involve four identical nucleotide changes at homologous sites in both exon duplicates. Our short reads from the genomes of *N. viridescens* and *Taricha* newts mapped onto each of these exon assemblies across putative recombination break points with high ($>$50-fold) coverage, lending support for sequence convergence rather than an assembly error. We did not detect gene conversion between these exons within the genomes of *T. granulosa* or *N. viridescens*; however, this may be due to the low power of GENECONV to detect conversion (Bay and Bielawski 2011), particularly in the presence of low sequence diversity and when the conversion tract is shorter than $\sim$100 bp (Posada and Crandall 2001; McGrath et al. 2009). Together, these results suggest that the three resistant amino acids
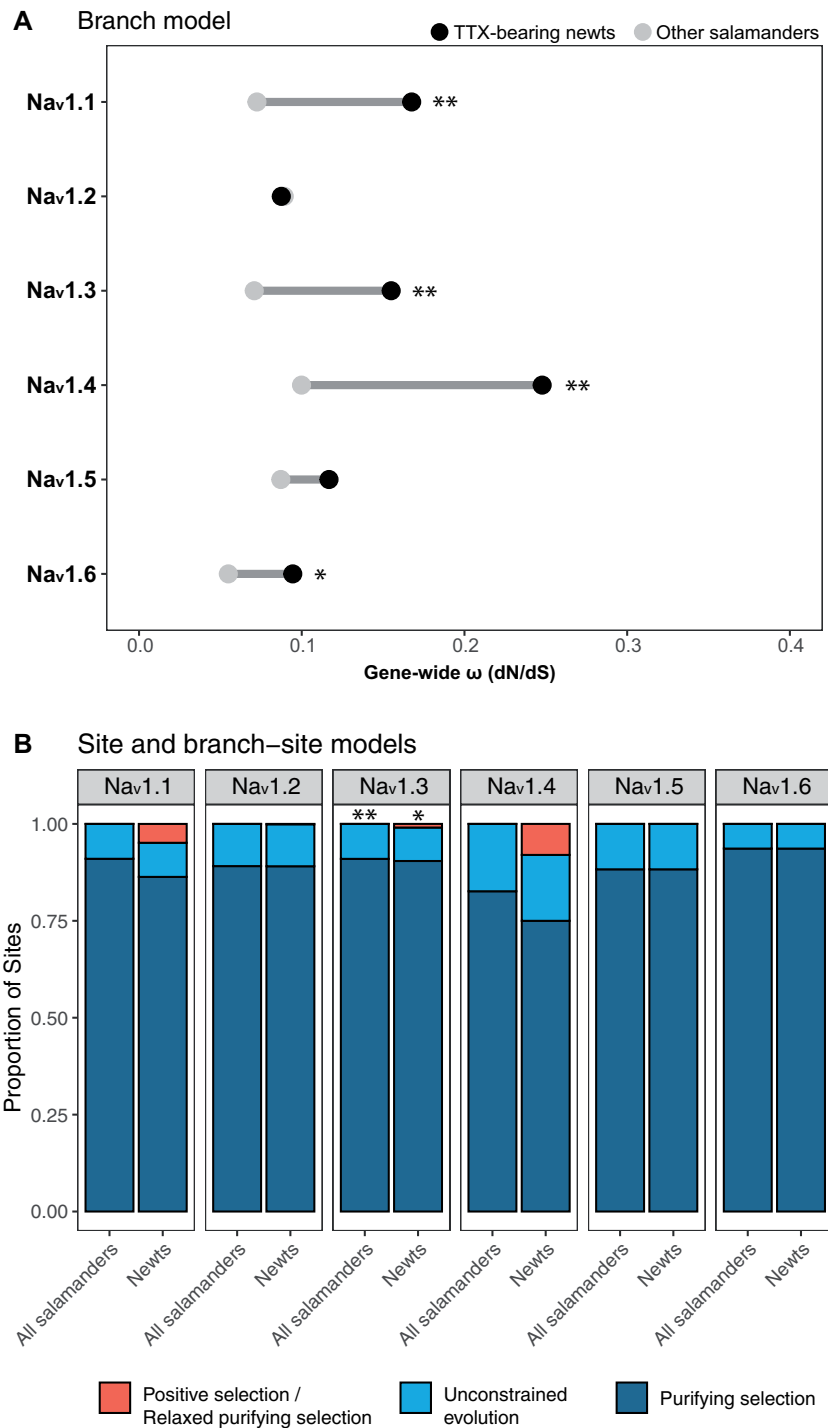
Fig. 4. Tests for shifts in selective pressure on salamander voltage-gated sodium channels. (A) PAML branch models comparing estimates of gene-wide ω (d_N/d_S) within TTX-bearing newts (black circles) and other salamanders (gray circles). (B) PAML site and branch-site model estimates of proportions of sites under purifying selection ($0 < \omega < 0.05$ in both lineages), unconstrained evolution ($\omega = 1$ in both lineages), and positive selection or relaxed purifying selection ($0 < \omega < 0.05$ in salamanders and $\omega \geq 1$ in TTX-bearing newts). Significant differences based on likelihood ratio tests are indicated with * ($P < 0.05$) and ** ($P < 0.01$). Although likelihood-ratio tests were nonsignificant for $Na_v1.1$ and $Na_v1.4$ (supplementary tables S3 and S4, Supplementary Material online), PAML identified a large proportion of amino acid coding sites within these paralogs with elevated d_N/d_S ratios in toxic newts.

accumulated together in one exon copy followed by conversion of the other exon $\sim$30 Ma in a toxic newt ancestor.

We also detected gene conversion between the DI P-loops of paralogs $Na_v1.1$ and $Na_v1.3$ within the genomes of both *Taricha* species (fig. 5B and table 5). TTX-resistant substitutions are identical in the DI P-loops of $Na_v1.1$ and $Na_v1.3$ in both *Taricha* species (401A, encoded by a GCT codon), whereas $Na_v1.1$ of *N. viridescens* contains a different codon

Table 4. P-Loop Sites with Elevated ω Values in All Salamanders and in Toxic Newts.

|	$Na_V1.1$	$Na_V1.2$	$Na_V1.3$	$Na_V1.4$	$Na_V1.5$	$Na_V1.6$
Tissue expression	Brain	Brain	Brain	Muscle	Heart	Brain/PNS
P-loop sites under positive selection in all salamanders[a,b]	Y401A/C (DI)[c] G1533V (DIV)[c]	G1533R (DIV)[c]	Y401A (DI)[c]	—	739 (DII)	Y401A (DI)[c]
P-loop sites under positive selection in toxic newts[b,d]	1224 (DIII) A1529G (DIV)[c]	—	T759S (DII)	W756Y (DII) M1240T (DIII)[c] 1517 (DIV) 1519 (DIV) D1532S (DIV)*,[a]	—	—

[a]Sites identified with site models using empirical Bayes method (posterior probability >0.50).
[b]Because we had low power to detect positive selection at specific sites due to the small number of species in our study, these results should be interpreted with caution.
[c]Nonconservative amino acid substitutions associated with TTX resistance in toxic newts.
[d]Sites identified with branch-site models using empirical Bayes method (posterior probability >0.50).
*Empirical Bayes posterior probability >0.95.
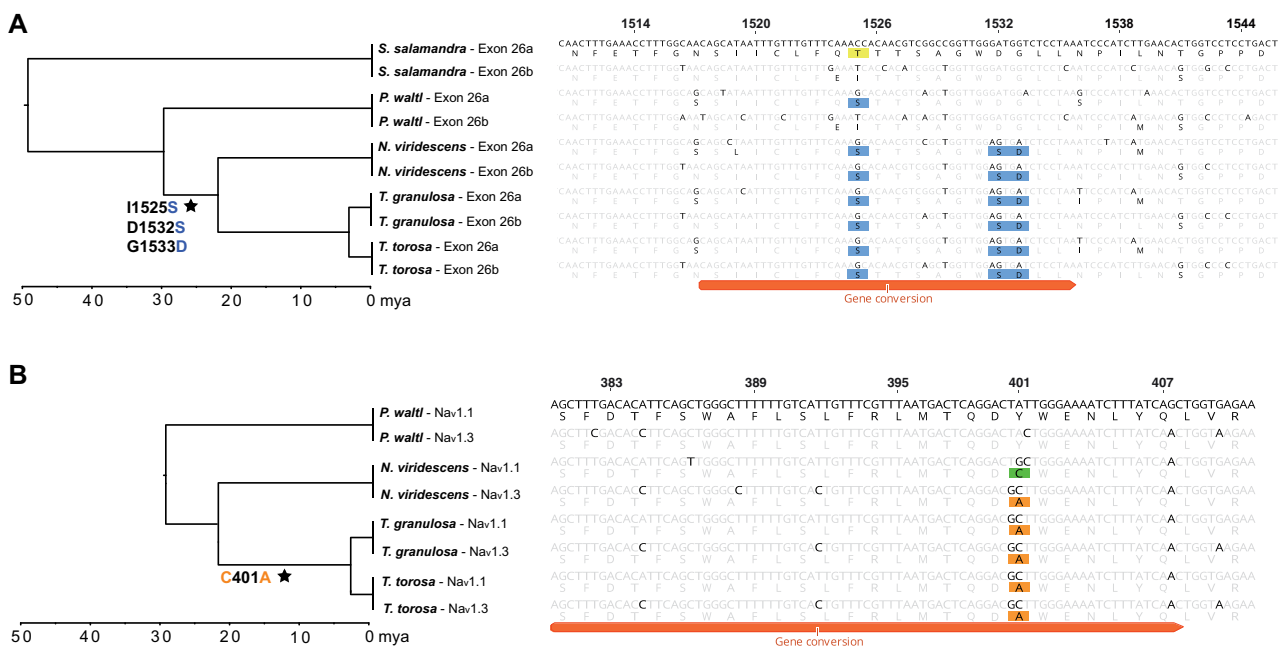
FIG. 5. Gene conversion within TTX-binding regions. (A) Gene conversion was detected between DIVa and DIVb P-loops within duplicate exons 26a and 26b of $Na_V1.4$ in *Taricha torosa*. Substitutions conferring TTX resistance are highlighted in yellow and blue. Although one moderately resistant substitution is present in DIVa of less toxic salamanders (1,525 T/S), three identical substitutions are present in both DIVa and DIVb of highly toxic newts. (B) Gene conversion was also detected between the DI P-loops of paralogs $Na_V1.1$ and $Na_V1.3$ in both *T. torosa* and *T. granulosa*. In *Notophthalmus*, both paralogs have different resistant substitutions (401C in $Na_V1.1$, highlighted in green; 401A in $Na_V1.3$, highlighted in orange). This putative gene conversion may have homogenized TTX-resistant substitutions among these paralogs within *Taricha* newts. Site numbers are in reference to amino acids of rat $Na_V1.4$ (accession number AAA41682). Stars at branches indicate the inferred transfer of substitutions associated with moderate resistance (blue text) or extreme resistance (orange text) via nonallelic gene conversion.

at this position (TGC, encoding 401C), consistent with gene conversion occurring at this locus in *Taricha*. Both $Na_V1.1$ and $Na_V1.3$ of nontetrodotoxic *Ple. waltl* newts encode a TTX-sensitive tyrosine at this locus. It is unclear whether putative gene conversion event(s) occurred before or after resistance evolved in both paralogs. Gene conversion may have converted a nonresistant channel to a resistant channel in an ancestral *Taricha*, whereas *N. viridescens* independently acquired a Y401A substitution, or it may have homogenized substitutions within two channels that had previously evolved resistance in an ancestor of all toxic newts. In

Taricha newts, the transition from either tyrosine or cysteine to alanine required multiple nucleotide substitutions in both paralogs, making gene conversion a likely explanation for the observed substitution patterns.

We detected additional gene conversion events that may have involved a nonresistant paralog acting as a donor to a resistant paralog, leading to the loss of TTX resistance in *A. mexicanum* and *C. alleganiensis* paralogs. A resistant substitution is present in the DIII P-loop of $Na_V1.1$ in most salamanders but is absent in $Na_V1.1$ of *A. mexicanum* (fig. 3), and we detected gene conversion in an adjacent region between

Table 5. Nonallelic Gene Conversion Events.

Na$_v$1.1–Na$_v$1.2–Na$_v$1.3 Coding Sequences

Species	Gene 1–Gene 2	BC P Value[a]	Protein Begin[b]	Protein End[b]	P-Loop	Exon	Length (bp)	Total Poly (bp)[c]	Num Diffs (bp)[d]	Total Diffs (bp)[e]
A. mexicanum	Na$_v$1.1–Na$_v$1.2	0.01	12	42	—	1	93	48	5	794
	Na$_v$1.1–Na$_v$1.3	0.01	45	84	—	1	128	54	5	722
	Na$_v$1.2–Na$_v$1.3	0.00	203	405	DI	5; 6; 7; 8	>626	74	2	902
	Na$_v$1.1–Na$_v$1.2	0.00	1,059	1,193	—	19; 20; 21	>407	134	25	794
	Na$_v$1.1–Na$_v$1.3	0.02	1,104	1,144	—	20	127	37	1	722
	Na$_v$1.1–Na$_v$1.2[f]	0.02	1,208	1,232	DIII	21	84	35	2	794
C. alleganiensis	Na$_v$1.1–Na$_v$1.2	0.00	1,111	1,232	DIII	20; 21	>376	153	23	621
	Na$_v$1.2–Na$_v$1.3[f]	0.02	1,478	1,611	DIV	26	406	164	32	693
	Na$_v$1.1–Na$_v$1.2	0.00	1,531	1,652	DIV	26	371	177	27	621
N. viridescens	Na$_v$1.1–Na$_v$1.3	0.00	500	512	—	10	89	41	1	733
	Na$_v$1.1–Na$_v$1.2	0.01	1,104	1,199	—	16	292	109	20	796
P. cinereus	Na$_v$1.1–Na$_v$1.2	0.00	12	32	—	1	64	31	0	838
	Na$_v$1.1–Na$_v$1.3	0.00	362	499	DI	8; 9; 10	>576	88	13	786
	Na$_v$1.2–Na$_v$1.3	0.02	573	599	—	13	83	29	2	897
	Na$_v$1.1–Na$_v$1.3	0.00	610	667	—	14	177	68	8	786
	Na$_v$1.1–Na$_v$1.2	0.00	1,135	1,305	DIII	20; 21; 22; 23; 24	>524	138	9	838
	Na$_v$1.1–Na$_v$1.3	0.03	1,430	1,473	—	26	134	46	5	786
P. waltl	Na$_v$1.1–Na$_v$1.3	0.03	1,369	1,386	—	25	56	30	0	738
T. granulosa	Na$_v$1.1–Na$_v$1.3[g]	0.01	374	408	DI	8	105	41	2	725
T. torosa	Na$_v$1.1–Na$_v$1.3[g]	0.01	374	408	DI	8	105	41	2	725

Na$_v$1.4 Exon 26

Species	Gene	BC P Value[a]	Protein Begin[b]	Protein End[b]	P-Loop	Exon	Length (bp)	Total Poly (bp)[c]	Num Diffs (bp)[d]	Total Diffs (bp)[e]
P. cinereus	Na$_v$1.4	0.01	1,509	1,534	DIV	26a–26b	77	26	0	154
T. torosa	Na$_v$1.4[g]	0.02	1,518	1,536	DIV	26a–26b	56	22	1	178

[a] Global Bonferroni-corrected (BC) P values from 10,000 simulations.
[b] Protein begin and end sites are in reference to the rat Na$_v$1.4 channel (accession number AAA41682).
[c] Polymorphism within the converted region across all species.
[d] Pairwise differences between the two paralogs within the converted region.
[e] Total pairwise differences across the entire length of the two paralogs.
[f] Putative gene conversion events associated with the loss of TTX resistance.
[g] Putative gene conversion events associated with the gain of TTX resistance.

Na$_v$1.1 and the nonresistant Na$_v$1.2 paralog within the *A. mexicanum* genome (table 5 and supplementary fig. S10A, Supplementary Material online). Similarly, *C. alleganiensis* Na$_v$1.2 contains a nonresistant 1533G within DIV of all six paralogs, whereas Na$_v$1.2 of *X. tropicalis* frogs encodes a putatively TTX-resistant 1533L, and gene conversion between paralogs Na$_v$1.2 and Na$_v$1.3 may have facilitated the loss of this substitution in salamanders (supplementary fig. S10B, Supplementary Material online).

Discussion

Here, we show that TTX-bearing newts have evolved resistance to their own toxicity through multiple parallel changes in their Na$_v$ genes and that, similar to snakes that consume TTX-containing prey (McGlothlin et al. 2016; Perry et al. 2018), some of the resistance in this taxon is ancient, first appearing in an early salamander. However, although substitutions conferring moderate TTX resistance are present in some nontoxic salamander genomes, only the TTX-bearing newts have substitutions conferring high resistance across all six of their Na$_v$ paralogs, and several of these channels harbor multiple resistant substitutions in more than one domain. Many of the substitutions conferring resistance to toxic newts

are also present in Na$_v$ paralogs of TTX-resistant pufferfish (Jost et al. 2008) and snakes (McGlothlin et al. 2016). Similar to pufferfish, newts appear to require resistance within all of their brain/nerve channels in addition to their hearts and muscles. This feature apparently distinguishes toxic prey from their predators, whose brain channels lack resistant substitutions (McGlothlin et al. 2014). This molecular parallelism emphasizes the strong structural and functional constraints on this gene family, which appear to limit the evolution of TTX resistance to a small number of predictable pathways, leading to convergent and parallel changes across multiple taxa (Feldman et al. 2012). We show that the evolution of extreme TTX resistance is accompanied by a shift in signatures of selection in four out of six paralogs, with suggestive evidence of positive selection acting directly on TTX-binding sites. Finally, the evolution of physiological resistance appears to have been facilitated by at least two instances of nonallelic gene conversion, which acted to introduce TTX-resistance substitutions from one paralog (or exon duplicate) to another, providing a rare example of the facilitation of adaptive evolution via nonallelic gene conversion.

Our reconstruction of the history of TTX resistance in salamanders reveals the ancient origins of moderate

resistance in nerve channels Na$_v$1.1 and Na$_v$1.6 and high resistance in the heart channel Na$_v$1.5, which arose ~160 Ma. Resistant substitutions in the muscle channel Na$_v$1.4 evolved later, becoming fixed in the clade including all newts and *S. salamandra* between 75 and 130 Ma. This was followed by the accumulation of additional substitutions in DIII, DIVa, and DIVb of Na$_v$1.4 within members of the highly toxic newt clade, providing their muscles with resistance to much higher concentrations of TTX relative to salamanders lacking these mutations (Hanifin and Gilly 2015). Substitutions in DI conferring extreme TTX resistance to the brain/nerve channels Na$_v$1.1, Na$_v$1.2, Na$_v$1.3, and Na$_v$1.6 also evolved more recently (~30 Ma) and they are limited to the toxic newt clade with only one exception, Na$_v$1.1 of *P. cinereus*, which may have arisen independently in this lineage. Toxic newts also have unique substitutions in DIV of Na$_v$1.1 and Na$_v$1.2, which may provide additional resistance to their brain channels or may compensate for structural or functional changes resulting from resistant substitutions in DI or in other regions of the protein. The widespread presence of TTX in modern newts suggests that possession of TTX evolved in the common ancestor of this clade (Hanifin 2010). This is supported by our observation of shared TTX-resistance substitutions across all Na$_v$ paralogs in highly toxic newts. However, the highly toxic newts included in this study are limited to North American species and do not include Asian or European newts (e.g., *Cynops* and *Triturus* spp.) known to have TTX (Hanifin 2010). Sequencing the Na$_v$ genes of these species will reveal if extreme resistance in the nerve channels is specific to North American newts or arose earlier in an ancestral newt species.

Whether the TTX-resistance substitutions observed in newt relatives are adaptive and what selective pressures act to retain them remains to be determined. In ancestral salamandrids, resistance in three or four of the six Na$_v$ proteins may have provided tolerance to low levels of TTX, facilitating the evolution of extreme toxicity in the modern newts, although it is unclear whether these substitutions arose in response to TTX exposure or as a side effect of selection for another aspect of channel function. Environmental exposure to TTX could potentially occur from TTX-bearing prey, such as terrestrial *Bipalium* flatworms (Stokes et al. 2014) or from TTX-producing bacteria (Vaelli et al. 2020). In a feeding study on *B. adventitium* flatworms, Ducey et al. (1999) demonstrated that although all salamanders rejected the flatworms when they were first presented, some habituated *Ambystoma* and *Plethodon* individuals were able to consume them with only minor symptoms of TTX poisoning, including apparent mucus production and numbing of the mouth. Although the amount of TTX present in the worms was not measured, this observation supports the conjecture that these substitutions play a protective role against consuming toxic prey.

Our power to detect sites undergoing positive selection was low due to the small number of species available for our analyses and the high sequence conservation among orthologs (Yang et al. 2000; Anisimova et al. 2001). However, our analyses provided evidence consistent with positive selection acting on TTX-binding sites, including sites implicated in the extreme TTX resistance of salamander muscle fibers. Our

branch models indicate that several Na$_v$ paralogs have higher ω ratios within the tetrodotoxic newt clade relative to other salamanders. This increase in ω ratio appears to be mainly the result of relaxed purifying selection rather than positive selection, as few sites were estimated to have $\omega > 1$ by branch-site models. Muscle channel Na$_v$1.4 had the highest ω ratio in toxic newts, coinciding with a relatively high proportion (~0.06) of sites detected as undergoing positive selection in toxic newts and purifying selection in other salamanders, although the likelihood ratio test was nonsignificant (supplementary table S4, Supplementary Material online). This pattern may derive from ongoing positive selection on Na$_v$1.4 resulting from the coevolutionary arms race between newts and snakes. Increased ω ratios in toxic newts coincide with the appearance of highly TTX-resistant substitutions within the DI P-loops of Na$_v$1.1, Na$_v$1.3, and Na$_v$1.6, DIV of Na$_v$1.1, and the DIII, DIVa, and DIVb P-loops in Na$_v$1.4. Although the pattern of these substitutions suggests that they are adaptive changes that occurred specifically within the tetrodotoxic newt clade, our branch-site models detected positive selection on TTX-binding sites only within the DIV P-loop of Na$_v$1.1 and the DIII and DIVa P-loops of Na$_v$1.4, whereas our site models detected positive selection on site 401 within paralogs Na$_v$1.1, Na$_v$1.3, and Na$_v$1.6 of all salamanders. This may be due to the statistically conservative nature of the branch-site model and the tendency of PAML to detect ongoing diversifying selection rather than rare positive selection events (Yang and dos Reis 2011). Furthermore, the site and branch-site models do not distinguish between biochemically conservative and nonconservative amino acid changes. Nevertheless, the detection of relatively high ω ratios within the toxic newt clade along with site-specific positive selection at known TTX-binding sites provides strong evidence that these substitutions are adaptive.

In addition to the six Na$_v$ paralogs described in amphibians (Zakon 2012), our sequence data revealed the presence of a partial duplication of the Na$_v$1.4 gene in salamanders that includes the entirety of exon 26, encoding the DIV P-loop, which likely occurred in an ancestor of Salamandroidea. The maintained open reading frame and shared expression patterns of transcripts encoding exons 26a and 26b in *A. mexicanum* tissues suggests that this duplicate region is functional in salamander muscles. In some insects that feed on toxic plants, the appearance of resistance-conferring substitutions is accompanied by one or more duplications of the genes that the toxin targets (Zhen et al. 2012; Petschenka et al. 2017). Petschenka et al. (2017) show that in at least one species, such gene duplication precedes resistance, and they suggest that gene duplication may help to alleviate the potential decrease in fitness incurred by the insects due to the negative pleiotropic effects of toxin-resistant mutations. Similarly, resistance in DIV of salamander Na$_v$1.4 appears after the duplication of this domain, and only the TTX-bearing newts have resistant substitutions in both exon copies, lending support to this hypothesis and raising the possibility that the evolution of physiological resistance in salamanders may have been mediated in part by this genomic novelty.

We observed a rare case of the generation of adaptive variants via nonallelic gene conversion, which occurred both between the duplicated exons of $Na_v1.4$ and between paralogs $Na_v1.1$ and $Na_v1.3$. Gene conversion is often thought to play a role in constraint, preserving the core functions of gene families (Chapman et al. 2006) and reducing deleterious mutation loads (Ohta 1989; Khakhlova and Bock 2006), and has also been associated with the diversification of major histocompatibility complex genes in mammals (Kuhner et al. 1991; Go et al. 2003) and the introduction of deleterious nonsynonymous mutations into different parts of the genome (Galtier et al. 2009; Casola et al. 2012). However, the potential for gene conversion to facilitate adaptation is less widely appreciated. Theory suggests that gene duplication and subsequent gene conversion may allow for movement between adaptive peaks via the accumulation of beneficial mutations in one gene copy that can be transferred to a favorable genetic background (Hansen et al. 2000). This process has been implicated in the adaptive evolution of hypoxia tolerance in high-altitude Tibetan wolves (Signore et al. 2019) and in heavy metal tolerance in *Arabidopsis* (Hanikenne et al. 2013). We observed a rare case of the generation of adaptive variants via nonallelic gene conversion, which occurred both between the duplicated exons of $Na_v1.4$ and between paralogs $Na_v1.1$ and $Na_v1.3$. In the brain channel genes $Na_v1.1$ and $Na_v1.3$, this likely occurred between two genes that had previously evolved resistance, homogenizing the substitutions between the two paralogs in *Taricha* newts. In the muscle channel gene $Na_v1.4$, three identical amino acids were present within both duplicated DIV TTX-binding domains in toxic newts, whereas only one resistant amino acid was present in a single DIV domain in their nontetrodotoxic salamander relatives, suggesting that resistant substitutions accumulated in one exon copy in a toxic newt ancestor and subsequently spread to the other exon copy via gene conversion. Both Hanifin and Gilly (2015) and Du et al. (2009) have shown that the single resistant amino acid observed in less toxic salamanders confers only low levels of TTX resistance, whereas the combination of the three amino acids found in highly toxic newts confers extreme resistance. As splice variants encoding the alternative exons appear to share similar expression patterns in salamanders, both exon copies should require extreme resistance in species exposed to high TTX concentrations. The concerted evolution of TTX resistance among homologous P-loop domains of $Na_v1.4$ may have expedited the evolution of extreme resistance in newt muscles, requiring new resistant mutations to appear in only one of these domains before being transferred to the other copy.

The degree of parallel molecular evolution among members of the Na_v gene family and across lineages provides insight into the constraints on Na_v nucleotide sequence as well as the evolvability of the TTX-resistance phenotype. Our results reveal that similar to their coevolutionary partners, *Thamnophis* garter snakes, *Taricha* newts evolved extreme TTX resistance through a stepwise process that built upon ancient changes that were in place millions of years before the arms race began. However, the pattern of TTX resistance evolution in newts also displays important differences from

that of their predators. First, perhaps because of the constitutive presence of TTX, newts display extreme levels of resistance even in channels that are expressed in the central nervous system, which are protected by the blood-brain barrier in species that encounter TTX in their diet. Second, our analysis indicates that many substitutions may have become fixed relatively close to one another in evolutionary time within the clade of modern newts. This is in contrast to snakes, where key changes were separated by millions of years. Due to our lack of sampling of newt species outside of North America, however, further work is necessary to understand the timing of these changes on a finer scale. We also show that although positive selection appears to be a strong driving force of the evolution of TTX auto-resistance in newts, gene conversion may have sped up the process of adaptive evolution in some Na_v paralogs, and constraints have limited the possible locations and types of resistant substitutions to a small subset of realized genetic changes. Taken together, our results emphasize the interplay among selection, constraint, and historical contingency in the evolution of complex adaptations.

Materials and Methods

Sequencing and Annotation of Voltage-Gated Sodium Channel Paralogs

We identified Na_v genes in the two publicly available salamander genome assemblies, *A. mexicanum* (Smith et al. 2019; AmexG.v6 assembly) and *Ple. waltl* (Elewa et al. 2017), and in one full-body transcriptome from the fire salamander *S. salamandra* (Goedbloed et al. 2017; BioProject accession number PRJNA607429) using the reciprocal best BLAST hit method (Moreno-Hagelsieb and Latimer 2008) with queries of Na_v sequences from *X. tropicalis* (Hellsten et al. 2010) and salamanders (Hanifin and Gilly 2015). We confirmed assignments of each amphibian Na_v paralog based on nucleotide alignments of the coding sequences with *Xenopus* sequences, as well as synteny of the chromosomal segments containing Na_v genes (supplementary fig. S1, Supplementary Material online). These Na_v annotations were then used to design targeted sequencing probes and to subsequently assign paralog identity to our de novo salamander assemblies. We used Geneious v10.2.3 for sequence visualization and to create DNA and protein alignments (Kearse et al. 2012). We also performed BlastN searches of published transcriptome assemblies of *Tyl. wenxianensis* (PRJNA323392), *B. vallecula* (PRJNA419601), and *H. retardatus* (Matsunami et al. 2015; PRJDB2409). However, we were unable to identify the full set of Na_v paralogs within these three assemblies, possibly due to their tissue specificity. Therefore, we used the sequences for probe design and to identify exon duplications in $Na_v1.4$ but excluded them from PAML analyses.

In order to design targeted sequencing probes, we compiled partial and complete amphibian Na_v sequences obtained from NCBI databases and additional published sources (supplementary table S7, Supplementary Material online) into a single FASTA file. Each individual FASTA entry included a single exon and, when available, up to 200 bp of intron

sequence upstream and downstream of each exon to aid in paralog assignment. Using RepeatMasker (Smit et al. 2013–2015), we replaced transposable elements and other sequence repeats with Ns, and subsequently filtered out sequences <120 bp in length, as well as those with more than 25% missing or ambiguous characters. We submitted this masked and filtered file, which was 465 kb in total length, to Agilent Technologies (Santa Clara, CA) for custom probe design using the SureSelect tool, resulting 7518 unique 120-mer probes. Probe sequences are available in our Dryad repository.

We obtained DNA samples from adult individuals of three TTX-bearing species ($n = 3$ for each species): *T. torosa* from Hopland, CA, *T. granulosa* from Benton, OR, and *N. viridescens* from Mountain Lake, VA, and from two additional salamander species presumed to lack TTX ($n = 2$ for each species): *P. cinereus* collected in Mountain Lake, VA and *C. alleganiensis* collected in southwestern VA. We extracted genomic DNA using the DNeasy Blood & Tissue kit (Qiagen Inc., Valencia, CA) and prepared sequencing libraries using the SureSelect^XT Target Enrichment system for Illumina paired-end multiplexed sequencing from Agilent Technologies (Santa Clara, CA), following the protocol for low input (200 ng) DNA samples. We used a Covaris M220 Focused-ultrasonicator to shear 200 ng of purified whole genomic DNA from each sample into ∼250 bp fragments using the following settings: duty factor 10%, peak incident power 75 w, 200 cycles per burst, and treatment time of 160 seconds. We followed the Agilent SureSelect^XT Target Enrichment kit protocol for end repair, adaptor ligation, amplification, hybridization, and bead capture (using the custom SureSelect probes described above), indexing, and purification. We quantified the resulting enriched, indexed libraries with qPCR, and combined them in equimolar concentrations into one final library pool, which was submitted to the Genomics Sequencing Center at Virginia Tech for sequencing on an Illumina MiSeq 300-cycle v2 with 150 bp paired-end reads. Prior to alignment, we trimmed Illumina reads of TruSeq3 adapter sequences, removed bases with a phred64 quality score less than 3, and filtered out subsequent reads shorter than 100 bp using Trimmomatic version 0.33 (Bolger et al. 2014). We used SPAdes 3.6.0 (Bankevich et al. 2012) to create de novo assemblies of the trimmed and filtered reads. Each Na_v paralog had >10-fold sequence coverage, with an average of 32-fold coverage across all species and paralogs (supplementary table S1, Supplementary Material online). After filtering, all reads had Phred Q-scores >30 for >99% of sites.

Because we designed the sequencing probes to capture only small portions of the Na_v intronic regions flanking exons (regions more likely to be conserved across species), each exon was assembled into a separate scaffold. For each individual from our sequencing trial, we created BLAST databases from the assembled de novo scaffolds and performed BLAST searches using single exons from the *Ambystoma* Na_v genes as queries. We created 26 separate nucleotide alignments, one for each individual Na_v exon, including sequences from *Ambystoma*, *Pleurodeles*, and our de novo assemblies using MAFFT v 7.450 (Katoh and Standley 2013) and created

consensus neighbor-joining trees with a Tamura–Nei genetic distance model using the Geneious Tree Builder (Kearse et al. 2012) with 1,000 bootstrap replicates and an 80% support threshold. The resulting tree topologies were used to assign paralog identity to each of the exons. When necessary, we included exon and intron sequences from additional species in the alignments to resolve the topology of the trees.

We concatenated all exons from each paralog into full coding sequences. Based on alignment with full-length *Xenopus* sequences, all salamander Na_v coding sequences collected for this study were >90% complete with the exception of two sequences from the *S. salamandra* transcriptome (paralogs Na_v1.1 and Na_v1.2, which were 68.8% and 70.7% complete, respectively; supplementary table S1, Supplementary Material online). For each species, we used Na_v paralogs sequenced from the genome of a single individual for our downstream analyses, based on completeness of the assembly.

Determination of TTX Resistance Levels

TTX sensitivity is commonly measured in vitro by using site-directed mutagenesis to introduce mutations of interest into a TTX-sensitive Na_v channel, followed by expression in *Xenopus* oocyte or HEK 293 cells and the application of patch-clamp whole-cell recordings to measure channel current in the presence of TTX. The fold change in TTX sensitivity is then calculated by taking the ratio of the IC_{50} values, or the TTX concentration at which 50% of the Na_v channels are blocked, of mutated and wild-type channels (see table 3 for references).

Another line of evidence for resistance in salamander muscle channels (Na_v1.4) comes from Hanifin and Gilly (2015), who estimated TTX sensitivity by recording action potentials generated from salamander muscle fibers and estimating the amount of TTX required to diminish the rise of the action potential, associating these relative changes with the presence and absence of substitutions in TTX-binding sites. They associated moderate TTX resistance (reduced sensitivity to 0.010 μM TTX) with the presence of DIII substitution M1240T and extreme resistance (low sensitivity to 300 μM TTX) with the presence of DIII and DIV substitutions M1240T, D1532S, and G1533D. We categorize levels of TTX resistance conferred by Na_v substitutions as extreme or moderate based on the results of Hanifin and Gilly (2015) as well as the data summarized in table 3.

Phylogenetic Analyses and Identification of Site-Specific Evolutionary Rates

We constructed phylogenetic trees for the entire Na_v gene family using our de novo assembled sequences as well as sequences from the genomes of *A. mexicanum*, *Ple. waltl*, the whole-body transcriptome of *S. salamandra*, two frog genomes: *X. tropicalis* (Hellsten et al. 2010) and *Nan. parkeri* (Sun et al. 2015), and one fish genome: *Danio rerio* (Howe et al. 2013). We created an amino acid alignment of translated coding sequences using MAFFT v 7.450 (Katoh and Standley 2013) and constructed maximum likelihood trees from these alignments with RAxML v8.2.11 (Stamatakis 2014) in

Geneious using a GAMMA BLOSSUM62 protein model and estimated clade support with 100 bootstrap replicates. In order to improve the accuracy of the nucleotide alignment, we used this amino acid alignments to guide codon alignments with PAL2NAL v14 (Suyama et al. 2006). We identified the best fitting substitution models for the nucleotide alignment using jModelTest 2.1.10 v20160303 (Darriba et al. 2012) and constructed maximum likelihood trees of the coding sequences with RAxML v8.2.11. The two models with the lowest AIC scores were: 1) the transition model with unequal base frequencies, a gamma shape parameter, and some proportion of invariable sites (TIM2+I+G) and 2) a general time-reversible model with a gamma shape parameter and a proportion of invariable sites (GTR+I+G), which is nearly identical to TIM2+I+G, but includes two additional rate parameters (Posada 2008). Because the two models are nearly equivalent and both fit our data equally well, we chose the GTR+I+G model for its ease of implementation across different programs. We repeated these methods for each individual Na_v paralog for downstream analyses in PAML, excluding the sequences from the outgroup species *Nan. parkeri* and *D. rerio*. We estimated chronograms in figures 3 and 5 using the chronos() function of the ape v5.4-1 package in R using a phylogenetic tree from Pyron (2014) and divergence dates from Hime et al. (2021; see Dryad repository for R code).

We estimated synonymous (d_S) and nonsynonymous (d_N) substitution rates, as well as the d_N/d_S ratios (ω) for each paralog using codeml in PAML v4.8 (Yang 2007). In order to test for changes in selective regimes in the Na_v genes between salamanders and highly toxic newts (*Notophthalmus* and *Taricha* species), we fit the following models to our Na_v alignments: 1) one-ratio models (allowing for a single ω ratio among all sites and all branches of the phylogeny), 2) branch models (allowing for separate ω ratios for the foreground [toxic newts] and background [other salamanders]), 3) branch-site neutral models (allowing ω to vary both between toxic newts and other salamanders and among sites, with two possible categories: $0 < \omega < 1$ and $\omega = 1$), and 4) branch-site models (allowing ω to vary both between toxic newts and other salamanders and among sites, with three possible categories: $0 < \omega < 1$, $\omega = 1$, and $\omega > 1$, the latter being allowed only within toxic newts). To test for site-specific positive selection among all salamanders, we fit two sets of nested models: 1) discrete ω ratio models M1a vs. M2a, which allowing for ω to vary among sites, with either two possible categories: $0 < \omega < 1$ and $\omega = 1$ or three possible categories: $0 < \omega < 1$, $\omega = 1$, and $\omega > 1$; and 2) continuous ω ratio models M7, M8a, and M8, which fit ω ratios of sites into a beta distribution, with ncatG (the number of ω values in the beta distribution) set to 5. We used F3x4 codon models, which estimate individual nucleotide frequencies for each of the three codon positions, and allowed codeml to estimate ω and transition-transversion rates (κ). The outputs of these models were used to estimate and compare gene-wide ω between toxic newts and salamanders (one-ratio and branch models), to identify sites under positive selection in all salamanders (site and neutral site models), and to identify sites

under positive selection or with elevated ω in toxic newts relative to other salamanders (branch-site neutral and branch-site models). We also created ancestral sequence reconstructions by specifying RateAncestor = 1 within codeml configuration files. We report posterior probability estimates for ancestral sequence reconstructions using models with the highest likelihood scores (supplementary table S3, Supplementary Material online), which were the neutral site models (M8a) for all Na_v paralogs except $Na_v1.3$, for which the site selection model M8 had the most support (supplementary figs. S4–S9, Supplementary Material online). We performed all of the above analyses both including and excluding the two *S. salamandra* paralogs with a large number of gaps ($Na_v1.1$ and $Na_v1.2$). Maximum likelihood parameter estimates were largely congruent using these different data sets. Therefore, we present results from the gene trees including *S. salamandra* here.

Detection of Gene Conversion

We used the program GENECONV to detect potential non-allelic gene conversion events between Na_v paralogs. We used a full codon alignment of all six Na_v paralogs from seven of the eight salamanders included in the study (excluding *S. salamandra* due to missing data), but targeted our search to include only genes $Na_v1.1$, $Na_v1.2$, and $Na_v1.3$ within each species under the assumption that gene conversion is more likely to occur between closely related sequences that reside on the same chromosome. This increased the power of detecting gene conversion from multiple pairwise comparisons. We also performed a separate search for gene conversion events between duplicate exons 26a and 26b of $Na_v1.4$. For this analysis, we used a codon alignment of $Na_v1.4$ exons 26a and 26b from ten salamander species. We assigned a mismatch penalty using gscale = 1 and used corrected *P* values from 10,000 permutations to determine significance.

Data Availability

Newly generated sequences have been submitted to the SRA database in NCBI under BioProject accession number PRJNA732671. Sequence alignments and configuration files for GENECONV analyses have been archived in a Dryad repository at http://doi.org/10.5061/dryad.kprr4xh4v.

References

Anisimova M, Bielawski JP, Yang Z. 2001. Accuracy and power of the likelihood ratio test in detecting adaptive molecular evolution. *Mol Biol Evol.* 18(8):1585–1592.

Arbuckle K, Rodríguez de la Vega RC, Casewell NR. 2017. Coevolution takes the sting out of it: evolutionary biology and mechanisms of toxin resistance in animals. *Toxicon* 140:118–131.

Bankevich A, Nurk S, Antipov D, Gurevich AA, Dvorkin M, Kulikov AS, Lesin VM, Nikolenko SI, Pham S, Prjibelski AD, et al. 2012. SPAdes: a new genome assembly algorithm and its applications to single-cell sequencing. *J Comput Biol.* 19(5):455–477.

Bay RA, Bielawski JP. 2011. Recombination detection under evolutionary scenarios relevant to functional divergence. *J Mol Evol.* 73(5–6):273–286.

Benovoy D, Drouin G. 2009. Ectopic gene conversions in the human genome. *Genomics* 93(1):27–32.

Bolger AM, Lohse M, Usadel B. 2014. Trimmomatic: a flexible trimmer for Illumina sequence data. *Bioinformatics* 30(15):2114–2120.

Bricelj VM, Connell L, Konoki K, MacQuarrie SP, Scheuer T, Catterall WA, Trainer VL. 2005. Sodium channel mutation leading to saxitoxin resistance in clams increases risk of PSP. *Nature* 434(7034):763–767.

Brodie ED 3rd, Brodie ED Jr. 1990. Tetrodotoxin resistance in garter snakes: an evolutionary response of predators to dangerous prey. *Evolution* 44(3):651–659.

Brodie ED Jr, Ridenhour BJ, Brodie ED 3rd. 2002. The evolutionary response of predators to dangerous prey: hotspots and coldspots in the geographic mosaic of coevolution between garter snakes and newts. *Evolution* 56(10):2067–2082.

Bryant DM, Johnson K, DiTommaso T, Tickle T, Couger MB, Payzin-Dogru D, Lee TJ, Leigh ND, Kuo T-H, Davis FG, et al. 2017. A tissue-mapped axolotl de novo transcriptome enables identification of limb regeneration factors. *Cell Rep.* 18(3):762–776.

Caballero-Pérez J, Espinal-Centeno A, Falcon F, García-Ortega LF, Curiel-Quesada E, Cruz-Hernández A, Bako L, Chen X, Martínez O, Alberto Arteaga-Vázquez M, et al. 2018. Transcriptional landscapes of Axolotl (*Ambystoma mexicanum*). *Dev Biol.* 433(2):227–239.

Casola C, Hahn MW. 2009. Gene conversion among paralogs results in moderate false detection of positive selection using likelihood methods. *J Mol Evol.* 68(6):679–687.

Casola C, Zekonyte U, Phillips AD, Cooper DN, Hahn MW. 2012. Interlocus gene conversion events introduce deleterious mutations into at least 1% of human genes associated with inherited disease. *Genome Res.* 22(3):429–435.

Chapman BA, Bowers JE, Feltus FA, Paterson AH. 2006. Buffering of crucial functions by paleologous duplicated genes may contribute cyclicality to angiosperm genome duplication. *Proc Natl Acad Sci U S A.* 103(8):2730–2735.

Chen J-M, Cooper DN, Chuzhanova N, Férec C, Patrinos GP. 2007. Gene conversion: mechanisms, evolution and human disease. *Nat Rev Genet.* 8(10):762–775.

Darriba D, Taboada GL, Doallo R, Posada D. 2012. jModelTest 2: more models, new heuristics and parallel computing. *Nat Methods.* 9(8):772–772.

Drouin G. 2002. Characterization of the gene conversions between the multigene family members of the yeast genome. *J Mol Evol.* 55(1):14–23.

Du Y, Nomura Y, Liu Z, Huang ZY, Dong K. 2009. Functional expression of an arachnid sodium channel reveals residues responsible for tetrodotoxin resistance in invertebrate sodium channels. *J Biol Chem.* 284(49):33869–33875.

Ducey PK, Messere M, Lapoint K, Noce S. 1999. Lumbricid prey and potential herpetofaunal predators of the invading terrestrial flatworm *Bipalium adventitium* (Turbellaria: Tricladida: Terricola). *Am Midl Nat.* 141(2):305–314.

Elewa A, Wang H, Talavera-López C, Joven A, Brito G, Kumar A, Hameed LS, Penrad-Mobayed M, Yao Z, Zamani N, et al. 2017. Reading and editing the Pleurodeles waltl genome reveals novel features of tetrapod regeneration. *Nat Commun.* 8(1):2286.

Feldman CR, Brodie ED Jr, Brodie ED 3rd, Pfrender ME. 2012. Constraint shapes convergence in tetrodotoxin-resistant sodium channels of snakes. *Proc Natl Acad Sci U S A.* 109(12):4556–4561.

Fux JE, Mehta A, Moffat J, Spafford JD. 2018. Eukaryotic voltage-gated sodium channels: on their origins, asymmetries, losses, diversification and adaptations. *Front Physiol.* 9:1406.

Galtier N, Duret L, Glémin S, Ranwez V. 2009. GC-biased gene conversion promotes the fixation of deleterious amino acid changes in primates. *Trends Genet.* 25(1):1–5.

Geffeney SL, Brodie ED Jr, Ruben PC, Brodie ED 3rd. 2002. Mechanisms of adaptation in a predator-prey arms race: TTX-resistant sodium channels. *Science* 297(5585):1336–1339.

Geffeney SL, Fujimoto E, Brodie ED 3rd, Brodie ED Jr, Ruben PC. 2005. Evolutionary diversification of TTX-resistant sodium channels in a predator-prey interaction. *Nature* 434(7034):759–763.

Go Y, Satta Y, Kawamoto Y, Rakotoarisoa G, Randrianjafy A, Koyama N, Hirai H. 2003. Frequent segmental sequence exchanges and rapid gene duplication characterize the MHC class I genes in lemurs. *Immunogenetics* 55(7):450–461.

Goedbloed DJ, Czypionka T, Altmüller J, Rodriguez A, Küpfer E, Segev O, Blaustein L, Templeton AR, Nolte AW, Steinfartz S. 2017. Parallel habitat acclimatization is realized by the expression of different genes in two closely related salamander species (genus *Salamandra*). *Heredity (Edinb)* 119(6):429–437.

Graham AM, McCracken KG. 2019. Convergent evolution on the hypoxia-inducible factor (HIF) pathway genes EGLN1 and EPAS1 in high-altitude ducks. *Heredity (Edinb)* 122(6):819–832.

Hague MTJ, Stokes AN, Feldman CR, Brodie ED, Brodie ED. 2020. The geographic mosaic of arms race coevolution is closely matched to prey population structure. *Evol Lett.* 4(4):317–332.

Hanifin CT. 2010. The chemical and evolutionary ecology of tetrodotoxin (TTX) toxicity in terrestrial vertebrates. *Mar Drugs.* 8(3):577–593.

Hanifin CT, Gilly WF. 2015. Evolutionary history of a complex adaptation: tetrodotoxin resistance in salamanders. *Evolution* 69(1):232–244.

Hanikenne M, Kroymann J, Trampczynska A, Bernal M, Motte P, Clemens S, Krämer U. 2013. Hard selective sweep and ectopic gene conversion in a gene cluster affording environmental adaptation. *PLoS Genet.* 9(8):e1003707.

Hansen TF, Carter AJR, Chiu C-H. 2000. Gene conversion may aid adaptive peak shifts. *J Theor Biol.* 207(4):495–511.

Hellsten U, Harland RM, Gilchrist MJ, Hendrix D, Jurka J, Kapitonov V, Ovcharenko I, Putnam NH, Shu S, Taher L, et al. 2010. The genome of the western clawed frog *Xenopus tropicalis*. *Science* 328(5978):633–636.

Hime PM, Lemmon AR, Lemmon ECM, Prendini E, Brown JM, Thomson RC, Kratovil JD, Noonan BP, Pyron RA, Peloso PLV, et al. 2021.

Phylogenomics reveals ancient gene tree discordance in the amphibian tree of life. *Syst Biol*. 70(1):49–66.

Howe K, Clark MD, Torroja CF, Torrance J, Berthelot C, Muffato M, Collins JE, Humphray S, McLaren K, Matthews L, et al. 2013. The zebrafish reference genome sequence and its relationship to the human genome. *Nature* 496(7446):498–503.

Jeziorski MC, Greenberg RM, Anderson PAV. 1997. Cloning of a putative voltage-gated sodium channel from the turbellarian flatworm *Bdelloura candida*. *Parasitology* 115(3):289–296.

Jost MC, Hillis DM, Lu Y, Kyle JW, Fozzard HA, Zakon HH. 2008. Toxin-resistant sodium channels: parallel adaptive evolution across a complete gene family. *Mol Biol Evol*. 25(6):1016–1024.

Katoh K, Standley DM. 2013. MAFFT multiple sequence alignment software version 7: improvements in performance and usability. *Mol Biol Evol*. 30(4):772–780.

Kearse M, Moir R, Wilson A, Stones-Havas S, Cheung M, Sturrock S, Buxton S, Cooper A, Markowitz S, Duran C, et al. 2012. Geneious Basic: an integrated and extendable desktop software platform for the organization and analysis of sequence data. *Bioinformatics* 28(12):1647–1649.

Khakhlova O, Bock R. 2006. Elimination of deleterious mutations in plastid genomes by gene conversion. *Plant J*. 46(1):85–94.

Kosakovsky Pond SL, Frost SDW. 2005. Not so different after all: a comparison of methods for detecting amino acid sites under selection. *Mol Biol Evol*. 22(5):1208–1222.

Kuhner MK, Lawlor DA, Ennis PD, Parham P. 1991. Gene conversion in the evolution of the human and chimpanzee MHC class I loci. *Tissue Antigens* 38(4):152–164.

Leffler A, Herzog RI, Dib-Hajj SD, Waxman SG, Cummins TR. 2005. Pharmacological properties of neuronal TTX-resistant sodium channels and the role of a critical serine pore residue. *Pflugers Arch*. 451(3):454–463.

Losos JB. 2011. Convergence, adaptation, and constraint. *Evolution* 65(7):1827–1840.

Márquez R, Ramírez-Castañeda V, Amézquita A. 2019. Does batrachotoxin autoresistance coevolve with toxicity in *Phyllobates* poison-dart frogs? *Evolution* 73(2):390–400.

Maruta S, Yamaoka K, Yotsu-Yamashita M. 2008. Two critical residues in P-loop regions of pufferfish Na^+ channels on TTX sensitivity. *Toxicon* 51(3):381–387.

Matsunami M, Kitano J, Kishida O, Michimae H, Miura T, Nishimura K. 2015. Transcriptome analysis of predator- and prey-induced phenotypic plasticity in the Hokkaido salamander (*Hynobius retardatus*). *Mol Ecol*. 24(12):3064–3076.

McGlothlin JW, Chuckalovcak JP, Janes DE, Edwards SV, Feldman CR, Brodie ED Jr, Pfrender ME, Brodie ED 3rd. 2014. Parallel evolution of tetrodotoxin resistance in three voltage-gated sodium channel genes in *Thamnophis sirtalis*. *Mol Biol Evol*. 31(11):2386–2846.

McGlothlin JW, Kobiela ME, Feldman CR, Castoe TA, Geffeney SL, Hanifin CT, Toledo G, Vonk FJ, Richardson MK, Brodie ED, et al. 2016. Historical contingency in a multigene family facilitates adaptive evolution of toxin resistance. *Curr Biol*. (12):261616–1621.

McGrath CL, Casola C, Hahn MW. 2009. Minimal effect of ectopic gene conversion among recent duplicates in four mammalian genomes. *Genetics* 182(2):615–622.

Moreno-Hagelsieb G, Latimer K. 2008. Choosing BLAST options for better detection of orthologs as reciprocal best hits. *Bioinformatics* 24(3):319–324.

Nowoshilow S, Schloissnig S, Fei J-F, Dahl A, Pang AWC, Pippel M, Winkler S, Hastie AR, Young G, Roscito JG, et al. 2018. The axolotl genome and the evolution of key tissue formation regulators. *Nature* 554(7690):50–55.

Ohta T. 1989. The mutational load of a multigene family with uniform members. *Genet Res*. 53(2):141–145.

Perry BW, Card DC, McGlothlin JW, Pasquesi GIM, Adams RH, Schield DR, Hales NR, Corbin AB, Demuth JP, Hoffmann FG, et al. 2018. Molecular adaptations for sensing and securing prey and insight into amniote genome diversity from the garter snake genome. *Genome Biol Evol*. 10(8):2110–2129.

Petschenka G, Wagschal V, von Tschirnhaus M, Donath A, Dobler S. 2017. Convergently evolved toxic secondary metabolites in plants drive the parallel molecular evolution of insect resistance. *Am Nat*. 190(S1):S29–S43.

Posada D. 2008. jModelTest: phylogenetic model averaging. *Mol Biol Evol*. 25(7):1253–1256.

Posada D, Crandall KA. 2001. Evaluation of methods for detecting recombination from DNA sequences: computer simulations. *Proc Natl Acad Sci U S A*. 98(24):13757–13762.

Pyron RA. 2014. Biogeographic analysis reveals ancient continental vicariance and recent oceanic dispersal in amphibians. *Syst Biol*. 63(5):779–797.

Sawyer S. 1989. Statistical tests for gene conversion. *Mol Biol Evol*. 6(5):526–538.

Semple C, Wolfe KH. 1999. Gene duplication and gene conversion in the Caenorhabditis elegans genome. *J Mol Evol*. 48(5):555–564.

Signore AV, Yang Y-Z, Yang Q-Y, Qin G, Moriyama H, Ge R-L, Storz JF. 2019. Adaptive changes in hemoglobin function in high-altitude Tibetan canids were derived via gene conversion and introgression. *Mol Biol Evol*. 36(10):2227–2237.

Smit A, Hubley R, Green P. 2013–2015. RepeatMasker Open-4.0.

Smith JJ, Timoshevskaya N, Timoshevskiy VA, Keinath MC, Hardy D, Voss SR. 2019. A chromosome-scale assembly of the axolotl genome. *Genome Res*. 29(2):317–324.

Smith SD, Pennell MW, Dunn CW, Edwards SV. 2020. Phylogenetics is the new genetics (for most of biodiversity). *Trends Ecol Evol*. 35(5):415–425.

Soong TW, Venkatesh B. 2006. Adaptive evolution of tetrodotoxin resistance in animals. *Trends Genet*. 22(11):621–626.

Stamatakis A. 2014. RAxML version 8: a tool for phylogenetic analysis and post-analysis of large phylogenies. *Bioinformatics* 30(9):1312–1313.

Stokes AN, Ducey PK, Neuman-Lee L, Hanifin CT, French SS, Pfrender ME, Brodie ED 3rd, Brodie ED Jr. 2014. Confirmation and distribution of tetrodotoxin for the first time in terrestrial invertebrates: two terrestrial flatworm species (*Bipalium adventitium* and *Bipalium kewense*). *PLoS One* 9(6):e100718.

Storz JF. 2016. Causes of molecular convergence and parallelism in protein evolution. *Nat Rev Genet*. 17(4):239–250.

Sun YB, Xiong ZJ, Xiang XY, Liu SP, Zhou WW, Tu XL, Zhong L, Wang L, Wu DD, Zhang BL, et al. 2015. Whole-genome sequence of the Tibetan frog *Nanorana parkeri* and the comparative evolution of tetrapod genomes. *Proc Natl Acad Sci U S A*. 112(11):E1257–E1262.

Sunami A, Glaaser IW, Fozzard HA. 2000. A critical residue for isoform difference in tetrodotoxin affinity is a molecular determinant of the external access path for local anesthetics in the cardiac sodium channel. *Proc Natl Acad Sci U S A*. 97(5):2326–2331.

Suyama M, Torrents D, Bork P. 2006. PAL2NAL: robust conversion of protein sequence alignments into the corresponding codon alignments. *Nucleic Acids Res*. 34(Web Server Issue):W609–W612.

Tarvin RD, Borghese CM, Sachs W, Santos JC, Lu Y, O'Connell LA, Cannatella DC, Harris RA, Zakon HH. 2017. Interacting amino acid replacements allow poison frogs to evolve epibatidine resistance. *Science* 357(6357):1261–1266.

Toledo G, Hanifin C, Geffeney S, Brodie ED 3rd. 2016. Convergent evolution of tetrodotoxin-resistant sodium channels in predators and prey. *Curr Top Membr*. 78:87–113.

Vaelli PM, Theis KR, Williams JE, O'Connell LA, Foster JA, Eisthen HL. 2020. The skin microbiome facilitates adaptive tetrodotoxin production in poisonous newts. *eLife* 9:e53898.

Venkat A, Hahn MW, Thornton JW. 2018. Multinucleotide mutations cause false inferences of lineage-specific positive selection. *Nat Ecol Evol*. 2(8):1280–1288.

Venkatesh B, Lu SQ, Dandona N, See SL, Brenner S, Soong TW. 2005. Genetic basis of tetrodotoxin resistance in pufferfishes. *Curr Biol*. 15(22):2069–2072.

Widmark J, Sundström G, Ocampo Daza D, Larhammar D. 2011. Differential evolution of voltage-gated sodium channels in tetrapods and teleost fishes. *Mol Biol Evol.* 28(1):859–871.

Williams BL, Hanifin CT, Brodie ED Jr, Brodie ED 3rd. 2010. Tetrodotoxin affects survival probability of rough-skinned newts (*Taricha granulosa*) faced with TTX-resistant garter snake predators (*Thamnophis sirtalis*). *Chemoecology* 20(4):285–290.

Yang Z. 1998. Likelihood ratio tests for detecting positive selection and application to primate lysozyme evolution. *Mol Biol Evol.* 15(5):568–573.

Yang Z, dos Reis M. 2011. Statistical properties of the branch-site test of positive selection. *Mol Biol Evol.* 28(3):1217–1228.

Yang Z, Nielsen R, Goldman N, Pedersen A-MK. 2000. Codon-substitution models for heterogeneous selection pressure at amino acid sites. *Genetics* 155(1):431–449.

Yang Z, Wong WSW, Nielsen R. 2005. Bayes empirical Bayes inference of amino acid sites under positive selection. *Mol Biol Evol.* 22(4):1107–1118.

Yang ZH. 2007. PAML 4: phylogenetic analysis by maximum likelihood. *Mol Biol Evol.* 24(8):1586–1591.

Yu FH, Catterall WA. 2003. Overview of the voltage-gated sodium channel family. *Genome Biol.* 4(3):207.

Zakon HH. 2012. Adaptive evolution of voltage-gated sodium channels: the first 800 million years. *Proc Natl Acad Sci U S A.* 109(Suppl 1):10619–10625.

Zakon HH, Jost MC, Lu Y. 2011. Expansion of voltage-dependent Na$^+$ channel gene family in early tetrapods coincided with the emergence of terrestriality and increased brain complexity. *Mol Biol Evol.* 28(4):1415–1424.

Zhang J, Nielsen R, Yang Z. 2005. Evaluation of an improved branch-site likelihood method for detecting positive selection at the molecular level. *Mol Biol Evol.* 22(12):2472–2479.

Zhen Y, Aardema ML, Medina EM, Schumer M, Andolfatto P. 2012. Parallel molecular evolution in an herbivore community. *Science* 337(6102):1634–1637.